ATLAS NOTE

ATLAS-CONF-2012-001

January 24, 2012

Search for supersymmetry in events with four or more leptons and missing transverse momentum in pp collisions at $\sqrt{s} = 7$ TeV with the ATLAS detector

ATLAS Collaboration

Abstract

The results of a search for supersymmetric particles in final states with four or more leptons (electrons or muons) and missing transverse momentum with the ATLAS detector is presented. The analysis uses a sample corresponding to an integrated luminosity of 2.06 fb^{-1} of proton-proton data recorded in 2011 at a centre-of-mass energy of 7 TeV. With an inclusive selection, four events are observed, while 1.7±0.9 are expected from Standard Model processes. After applying a Z boson veto for leptons pairs with the same flavour and opposite charge, no events are observed for 0.7±0.8 events expected. Within the selection acceptance, we determine 95% C.L. visible cross-section upper limits for new phenomena of 3.5 fb and 1.5 fb for the selections without and with the Z boson veto, respectively.

1 Introduction

The Standard Model (SM) of elementary particles, despite its many successes, is known to be an incomplete theory with an unstable scalar sector at high energies. Supersymmetry (SUSY) [1–7] provides a solution for several of the shortcomings of the SM. It postulates the existence of a boson (fermion) "superpartner" for each of the SM fermions (bosons) with the same mass and couplings, effectively more than doubling the particle content of the theory. To avoid proton decay, a new quantum number denoted R-parity is introduced that is even (odd) for SM (SUSY) particles. If R-parity is conserved (RPC) [8, 9] SUSY particles are produced in pairs at the LHC and the lightest SUSY particle (LSP) is stable. In much of the SUSY parameter space, the LSP is the lightest neutralino, a massive weakly interacting neutral particle that would escape the ATLAS detector. As SUSY particles have not yet been observed, SUSY, if it exists, must be broken by an unknown mechanism, allowing the SUSY partners of the SM particles to take large masses. If these masses are within the reach of the LHC, squarks and gluinos can be abundantly produced. Multilepton signatures may then arise as a consequence of the squark and gluino decay cascades via charginos, neutralinos and sleptons. These latter particles can also be directly produced, though with lower cross-sections that fall rapidly with the particle mass.

Multilepton final states can also be produced in R-parity violating (RPV) [10] scenarios, where for example, a stau ($\tilde{\tau}$) decays into a τ lepton, two charged leptons and a neutrino via intermediate virtual SUSY particles. Both scenarios, RPC and RPV, lead to the production of significant missing transverse momentum in the event, which can be exploited to distinguish SUSY multilepton production from SM processes. Searches for multilepton final states have been performed at the LHC by the ATLAS [11, 12] and the CMS [13] experiments.

This analysis uses $2.06\,\text{fb}^{-1}$ of the LHC proton-proton collision data at a centre-of-mass energy ($\sqrt{s}$) of 7 TeV recorded by the ATLAS detector in 2011. The data were collected with a single electron trigger with a transverse energy (E_{T}) threshold that was raised from 20 GeV to 22 GeV for higher LHC luminosities or a single muon trigger with a transverse momentum (p_{T}) threshold of 18 GeV. The analysis is based on events with at least four leptons, for which the "four-lepton" shorthand is also used in the text. It should be noted that the term lepton here refers to electrons and muons only, including those originating from leptonic τ decays.

2 The ATLAS Detector

ATLAS [14] is a particle physics detector with a cylindrical geometry and near 4π coverage in solid angle[1]. The inner detector (ID) consists of a silicon pixel detector, a silicon microstrip detector, and a transition radiation tracker. The ID is surrounded by a thin superconducting solenoid providing a 2 T magnetic field, and by high-granularity liquid-argon (LAr) sampling electromagnetic calorimeters. Hadronic coverage is provided by an iron-scintillator tile calorimeter in the central rapidity range. The end-cap and forward regions are instrumented with LAr calorimeters for both electromagnetic and hadronic measurements. The muon spectrometer (MS) surrounds the calorimeters and consists of three large superconducting toroids, a system of precision tracking chambers, and detectors for triggering.

[1] ATLAS uses a right-handed coordinate system with its origin at the nominal interaction point in the centre of the detector and the z-axis coinciding with the axis of the beam pipe. The x-axis points from the nominal interaction point to the centre of the LHC ring, and the y-axis points upward. Cylindrical coordinates (r, ϕ) are used in the transverse plane, ϕ being the azimuthal angle around the beam pipe. The pseudorapidity is defined in terms of the polar angle θ as $\eta = -\ln\tan(\theta/2)$.

3 Monte Carlo Simulation and Modelling

Fully simulated Monte Carlo (MC) samples are generated to estimate the contributions from most of the SM processes relevant for the analysis presented here. Detector response is simulated [15] with a program based on GEANT4 [16].

MC@NLO [17] is used to simulate top-pair/single-top production with the next-to-leading-order parton density function (PDF) set CTEQ6.6 [18], and the cross-sections are normalised to approximate next-to-next-to-leading order (NNLO) [19–22]. Production of electroweak gauge bosons (W, Z, Z^*) accompanied by jets is simulated using ALPGEN [23] with the PDF set CTEQ6L1, and the cross-sections are normalised to NNLO [24, 25]. The $Z^{(*)}/\gamma$+jets samples have a generator level dilepton invariant mass cut of 40 GeV. Low-mass Z^*/γ^*+jets (referred to as Drell-Yan) samples are also simulated in the same manner, with the Z^*/γ^* mass ranging between 10–40 GeV. Diboson (WZ, ZZ and WW) events are simulated using HERWIG [26] with the MRST2007LO* PDF [27], and the cross-sections are normalised to NLO [28]. Top-pair production with an additional weak boson ($t\bar{t}V$, where V=W,Z) is simulated using the MC generator Madgraph [29] at tree level and PYTHIA [30] is used for showering. The $t\bar{t}V$ samples are simulated with the PDF set CTEQ6L1, and the cross-sections are normalised to NLO [31]. The SM diboson backgrounds from $Z/W + \gamma$ ($Z\gamma$,$W\gamma$) are also simulated using Madgraph and PYTHIA with the PDF set CTEQ6L1, and the cross-sections are normalised to LO [32]. Fragmentation and hadronisation for the ALPGEN and MC@NLO samples is performed with HERWIG, using JIMMY [33] for the underlying event.

RPC SUSY scenarios are simulated with Herwig++ [34], while RPV SUSY scenarios are simulated with Fortran Herwig [26]. These SUSY scenarios are used for event selection optimisation; however, they are not used to interpret the results presented in this note, which are given as visible signal cross-sections. Two benchmark SUSY models are displayed in figures: one an RPV SUSY scenario and the other an RPC SUSY scenario. The RPV scenario is defined by the SUSY parameters m_0, $m_{1/2}$, A_0, tanβ, sign(μ) and Λ, where m_0, $m_{1/2}$ are the universal supersymmetry-breaking scalar and gaugino masses, A_0 is the universal supersymmetry-breaking scalar trilinear coupling, tanβ is the ratio of the vacuum expectation values of the two Higgs fields and Λ refers to a choice of exactly one of the 36 dimensionless RPV couplings in the extended superpotential λ_{ijk} (where the indices stand for the generations involved). The RPV benchmark model [35] (labelled "RPV") is defined by $m_{1/2}$ =400 GeV, tanβ =22, m_0 =A_0 =0, sign(μ) =1 at the Grand Unified Theory scale and λ_{121} = 0.032 (0.048) at the Grand Unified Theory (electroweak) scale. For the RPV benchmark scenario considered here, the inclusive SUSY production cross-section is σ = 0.35 pb and the $\tilde{\tau}$ LSP decays via two virtual intermediate sparticles into a τ, electron, neutrino and either a muon or another electron, e.g. $\tilde{\tau} \to \tau(\tilde{\chi}_1^0)^* \to \tau\mu^+(\tilde{\mu}_L^-)^* \to \tau\mu^+e^-\bar{\nu}_e$. The RPC scenario (labelled "DGwSL" for "direct gauginos with sleptons") is defined by bino mass m_1 =100 GeV, wino mass m_2 =250 GeV, higgsino mass μ =160 GeV and tanβ =6 (which ensures sufficiently large branching ratios into first and second generation leptons). For this set of parameters, the dominant process is the associated production of charginos and neutralinos with sleptons in the decay chain. In particular, the production of $\tilde{\chi}_2^0\tilde{\chi}_2^0$ dominates for a four-lepton final state where $\tilde{\chi}_2^0 \to \ell^\pm\tilde{\ell}_R^\mp \to \ell^\pm\ell^\mp\tilde{\chi}_1^0$. In the RPC benchmark model, the inclusive SUSY production cross-section is σ =2.84 pb, reduced to σ =1.50 pb after a two-lepton (e,μ,τ $p_{\mathrm{T}} > 7$ GeV) generator filter is applied. For the RPC scneario considered here, the neutralino masses are $m(\tilde{\chi}_1^0,\tilde{\chi}_2^0,\tilde{\chi}_3^0,\tilde{\chi}_4^0)$ = (81, 147, 168, 290) GeV, the chargino masses are $m(\tilde{\chi}_1^\pm,\tilde{\chi}_2^\pm)$ = (131, 290) GeV and the slepton mass is $m(\tilde{\ell}_R)$ = 106 GeV. It should be noted, other RPC scenarios may feature $m(\tilde{\ell}) > m(\tilde{\chi})$, where the $\tilde{\chi}_2^0$ can decay via $\tilde{\chi}_2^0 \to Z^{(*)}\tilde{\chi}_1^0 \to \ell^\pm\ell^\mp\tilde{\chi}_1^0$.

4 Event Reconstruction and Selection

Electrons in the signal region are required to pass selection criteria based on shower shape in the calorimeters, the quality of the track and the track-cluster matching [36]. They must have $E_{\mathrm{T}} > 10\,\mathrm{GeV}$ and $|\eta| < 2.47$ or $E_{\mathrm{T}} > 15\,\mathrm{GeV}$ for the barrel/end-cap transition region where $1.37 < |\eta| < 1.52$. Electrons are required to be well isolated, with the ratio of the summed p_{T} of other ID tracks within a cone $\Delta R = \sqrt{(\Delta\eta)^2 + (\Delta\phi)^2} < 0.2$ around the electron track to the electron's transverse energy less than 0.1. Electron candidates with an associated calorimeter cluster in a region with a local LAr calorimeter read-out problem are rejected with $\sim 1\%$ loss of acceptance for electrons.

Muons are required to be identified either in both the ID and MS systems (combined muons) or as a match between an extrapolated ID track and one or more track segments in the MS. Only muons with $p_{\mathrm{T}} > 10\,\mathrm{GeV}$ and $|\eta| < 2.4$ are considered. Muons are required to be isolated, with the summed p_{T} of other ID tracks within a distance $\Delta R < 0.2$ around the muon track less than 1.8 GeV and the total transverse energy in the calorimeter within $\Delta R < 0.3$ of the muon less than 4 GeV.

Jets are reconstructed using the anti-k_t jet clustering algorithm [37] with a radius parameter $R = 0.4$. The inputs to this algorithm are clusters of calorimeter cells seeded by cells with energy significantly above the measured noise. Jets are constructed by performing a four-vector sum over these clusters, treating each cluster as an (E, p) four-vector with zero mass. Jets are corrected for calorimeter non-compensation, dead material and other effects using p_{T}- and η-dependent calibration factors obtained from MC simulation and validated with test-beam and collision data [38]. Only jets with $p_{\mathrm{T}} > 20\,\mathrm{GeV}$ and $|\eta| < 2.8$ are considered.

If a jet and an electron are both identified within $\Delta R < 0.2$ of each other, the jet is discarded. Furthermore, identified electrons or muons are discarded if the separation from the closest remaining jet is $\Delta R < 0.4$. Electrons and muons separated by $\Delta R < 0.1$ are both discarded.

The calculation of the missing transverse momentum, $E_{\mathrm{T}}^{\mathrm{miss}}$, is based on the modulus of the vector sum of the p_{T} of the reconstructed objects (jets with $p_{\mathrm{T}} > 20\,\mathrm{GeV}$, but over the full calorimeter coverage $|\eta| < 4.9$, and selected leptons), including non-isolated muons, and the calorimeter clusters not belonging to reconstructed objects.

Events are rejected if they contain any jet failing basic quality selection criteria. This rejects detector noise and non-collision backgrounds [39]. The primary vertex of the event is defined as the vertex with the largest squared sum of transverse momenta of associated tracks and must have at least five associated tracks. Events are rejected if they contain a cosmic muon candidate identified by a longitudinal impact parameter $|z_0| > 1$ mm or a transverse impact parameter $|d_0| > 0.2$ mm with respect to the primary vertex. To ensure a good trigger efficiency, events must have at least one electron or muon candidate above the threshold required for the trigger efficiency plateau (electron with $E_{\mathrm{T}} > 25\,\mathrm{GeV}$, muon with $p_{\mathrm{T}} > 20\,\mathrm{GeV}$).

Due to a local readout problem in the LAr calorimeter affecting ~42% of the data, events in that subset of data and a corresponding fraction of the MC simulation containing a jet with $p_{\mathrm{T}} > 40\,\mathrm{GeV}$ (corrected for bad cells) or an identified electron with $-0.1 < \eta < 1.5$ and $-0.9 < \phi < -0.5$ are rejected.

A range of SUSY scenarios can give rise to events with four or more leptons. The requirement of four or more leptons in the final state is strong enough to suppress practically all of the purely hadronic SM backgrounds typical of the LHC environment. Same-flavour opposite-sign (SFOS) lepton pairs with dilepton mass below 20 GeV are discarded to suppress Drell-Yan, $W/Z\gamma$ and photon conversion backgrounds. Diboson events (ZZ and, to a lesser extent, WZ) potentially still survive as background sources in this channel; however, a cut on the total missing transverse momentum ($E_{\mathrm{T}}^{\mathrm{miss}} > 50\,\mathrm{GeV}$) in the event provides effective rejection. Therefore, a first signal region, referred to as SR1, is defined by requiring four-leptons and $E_{\mathrm{T}}^{\mathrm{miss}} > 50\,\mathrm{GeV}$. A second signal region, referred to as SR2, is also defined, where, in addition to the four-lepton and missing transverse momentum requirements, a veto is placed on

events containing SFOS lepton pairs with invariant mass within ±10 GeV of the nominal Z boson mass. This Z boson veto is to remove SM background events for scenarios such as the RPV benchmark model, where Z bosons are not present in the decay chain. It should be noted that, apart from the lepton-jet separation, which can effect the selection of electrons and muons, no explicit requirements are made on jets in the signal regions. Results from both selections are shown in Section 7.

5 Background Estimation

In this paper, backgrounds to SUSY-inspired four-lepton searches are estimated using MC simulation and validated using control regions in data. Only backgrounds yielding at least two prompt leptons (those produced from $W/Z^{(*)}/\tau$ decays) are considered as backgrounds to this four-lepton SUSY search, as dedicated studies of W+jet MC simulation have shown backgrounds with less than two prompt leptons to contribute negligibly. Internal conversions ($Z \to \ell\ell\gamma^*$) are not described by the MC simulation used in this analysis and are estimated from data by measuring the probability for the virtual photon to convert into two leptons. The photon conversion probability is measured using the ratio of $\ell\ell\gamma$ events to $\ell\ell\ell\ell$ events with $m_{\ell\ell\gamma}$ and $m_{\ell\ell\ell\ell}$ within 10 GeV of the Z boson mass and $E_{\mathrm{T}}^{\mathrm{miss}} < 50$ GeV. The contribution to the signal regions from internal conversions is then estimated by applying the photon conversion rate measured in the low-$E_{\mathrm{T}}^{\mathrm{miss}}$ region to $\ell\ell\gamma$ events in the high-$E_{\mathrm{T}}^{\mathrm{miss}}$ region. Internal conversions are found to have a negligible contribution in the signal regions.

The background model is validated using $t\bar{t}$-rich and low-$E_{\mathrm{T}}^{\mathrm{miss}}$ ZZ-rich control samples. A $t\bar{t}$-rich four-lepton control region is defined by requiring the presence of an opposite-flavour opposite-sign lepton pair, a b-tagged jet and by reversing the isolation requirement on two of the four leptons. The b-tagging algorithm exploits both impact parameter and secondary vertex information and has an average b-tagging efficiency of ~60% in $t\bar{t}$ events [40]. Events with $E_{\mathrm{T}}^{\mathrm{miss}} > 50$ GeV are selected, where 8.4±0.8 (stat) events are predicted using MC simulation and 8 events are observed in data.

A ZZ-rich control region is defined by requiring four-leptons and $E_{\mathrm{T}}^{\mathrm{miss}} < 50$ GeV, for which 23±5 (stat+syst, as described in Section 6) events are predicted using MC simulation and 20 events are observed in data. Additional checks in other background-rich control regions (using reversed lepton isolation) also yield good agreement between data and MC simulation within uncertainties.

6 Systematic Uncertainties

A summary of the main systematic uncertainties for the signal regions SR1 and SR2 is given in Table 1. Systematic effects on the estimated number of SM background events include uncertainties in the jet and lepton energy scales and resolutions, in the scaling factors that account for differences between data and MC simulation for lepton efficiencies, in the theoretical fiducial cross-sections and luminosity used to normalise the processes, in the PDFs, and uncertainties due to the modelling of multiple pp collisions. Of these, the uncertainties in the jet energy scale and resolution as well as electron energy resolution are among the dominant ones, at approximately 20%, dominated by the low statistics remaining in the Z+(u,d,s jets) MC samples after applying the selection criteria (a single MC event remains). The MC modelling of the local readout problem in the LAr calorimeter for a subset of the data is studied by varying the 40 GeV p_{T} threshold of the jets used for the event rejection by 20% in MC simulation. The systematic uncertainty from the trigger efficiency is found to be negligible (<<1%). A 10% systematic uncertainty is applied to the $t\bar{t}$, single top, $t\bar{t}V$ and Z+(c,b jets) MC samples to account for differences in the lepton fake rate from heavy flavour meson decays in MC simulation and data, based on a tag-and-probe study in a $b\bar{b}$-rich region. The uncertainty in the intergrated luminosity is 3.7% [41, 42]. The uncertainty in MC simulation cross-sections used in this analysis is 5% for ZZ, WW, Z+(u,d,s jets)

Table 1: The total number of expected events and absolute systematic uncertanties in the signal regions SR1 and SR2.

	SR1	SR2
Expected Events	1.70	0.66
MC statistics	0.59	0.57
Jet Energy Scale	0.35	0.34
Jet Energy Resolution	0.34	0.34
Electron Energy Scale	0.07	0.03
Electron Energy Resolution	0.34	0.34
Muon Inner Detector Track p Resolution	0.01	0.00
Muon Spectrometer Track p Resolution	0.01	0.00
Electron ID/Reconstruction Efficiency	0.09	0.07
Muon ID/Reconstruction Efficiency	0.01	0.00
Multiple pp collisions	0.02	0.01
LAr readout problem	0.02	0.00
PDF	0.08	0.02
Factorisation/Normalisation Scale	0.11	0.06
Cross-sections	0.20	0.04
Luminosity	0.06	0.02
Heavy flavour lepton fake rate	0.05	0.01
TOTAL systematic error	0.88	0.82

and Drell-Yan [24, 28], $^{+7.0}_{-9.6}$% for $t\bar{t}$ [19, 43], 7% for single top [21, 22], 40% for $t\bar{t}V$ [31] and 7% for WZ [28]. For Z+(c,b jets) the uncertainty in the cross-section is 30–40% [25]; however, 100% is used here as the uncertainty is dependent on the event topology of the analysis. When calculating the total systematic uncertainty on the background estimation, the sources of systematic uncertainty are assumed to be uncorrelated.

7 Results

In SR1, four events are observed, while 1.7±0.9 events are expected from SM processes. Zero events are observed in SR2, with 0.7±0.8 events expected. The uncertainties given include all systematic uncertainties considered. A breakdown of the estimated SM backgrounds for each flavour combination and their sum before and after applying the $E_{\mathrm{T}}^{\mathrm{miss}}$ requirement is given in Table 2 and Table 3, respectively. Table 3 is split into the two signal regions. Only the total SM background contribution ("All" column) is used in the following for the purpose of setting exclusion limits. The uncertainties quoted for the "All" column are inclusive and not the summed uncertainties of the different flavour combinations. Where MC samples yield no events, an upper limit is applied to describe the uncertainty, based on the luminosity of the sample used: defined as $1.1\times\mathcal{L}^{\mathrm{data}}/\mathcal{L}^{\mathrm{MC}}$ (1.1 is the mean of the Poisson distribution for which zero events are seen with a 32% frequency or 1σ deviation). MC simulation studies using the high statistics available in low lepton multiplicity events show the Drell-Yan (m_{Z^*/γ^*} = 10–40 GeV) contribution is never more than 5% of the Z+jets contribution (all jet flavours included). We therefore assign an upper limit of 5% of the nominal Z+jets estimate plus its uncertainty to the Drell-Yan background expectation.

The agreement between observed and expected event yields, expressed as a *p-value*, is assessed using a profile likelihood method [44], which is also employed to compute upper limits on the visible cross-sections for new phenomena. The uncertainties in the SM estimates are therein treated as nuisance parameters with Gaussian likelihoods. The *p-value* for SR1 is 0.10, while the *p-value* for SR2 is >0.5. The SM background estimation describes the data sufficiently well, with CL_b values of 0.07 and 0.78 for

the inclusive channels in SR1 and SR2, respectively.

For the visible cross-sections for new phenomena, defined by the product of cross-section, branching ratio, efficiency and acceptance, we find using the CL_s method [45] observed (expected) upper limits of 3.5 (2.1) fb and 1.5 (1.5) fb for SR1 and SR2, respectively.

Table 2: Number of events at the four-lepton stage of the analysis, before the $E_{\mathrm{T}}^{\mathrm{miss}}$ requirement, for SM MC simulation and 2.06 fb^{-1} of 2011 data. The uncertainties quoted for the "All" column are inclusive and not the summed uncertainties of the different flavour combinations. Where MC samples yield zero events, the uncertainty is quoted based on the integrated luminosity of the MC sample (see text).

4ℓ events	All	$eeee$	$eee\mu$	$ee\mu\mu$	$e\mu\mu\mu$	$\mu\mu\mu\mu$
$t\bar{t}$	0.22±0.15	0.012±0.042	0.06±0.06	0.10±0.07	0.05±0.07	0±0.018
Single t	0±0.04	0±0.04	0±0.04	0±0.04	0±0.04	0±0.04
$t\bar{t}V$	0.59±0.26	0.086±0.043	0.14±0.07	0.17±0.08	0.13±0.06	0.07±0.04
ZZ	19±5	3.8±1.0	0.16±0.08	10.0±2.5	0.17±0.07	4.9±1.2
WZ	0.54±0.17	0.06±0.03	0.07±0.04	0.17±0.07	0.24±0.09	0±0.011
WW	0±0.015	0±0.015	0±0.015	0±0.015	0±0.015	0±0.015
$Z\gamma$	0±0.5	0±0.5	0±0.5	0±0.5	0±0.5	0±0.5
Z+(u, d, s jets)	3.8±1.6	1.8±0.9	0±0.29	1.5±1.1	0.6±0.6	0±0.29
Z+(c, b jets)	0.26±0.28	0.022±0.037	0.06±0.07	0.13±0.14	0.05±0.06	0.0021±0.0034
Drell-Yan	0±0.29	0±0.14	0±0.018	0±0.14	0±0.06	0±0.014
Σ SM	25±5	5.8±1.4	0.5±0.6	12.0±2.8	1.2±0.7	5.0±1.4
Data	24	8	2	8	0	6

The p_{T}-ordered transverse energy (or momentum) distributions of the four leptons before applying the $E_{\mathrm{T}}^{\mathrm{miss}}$ requirement are shown for data and MC simulation in Figures 1(a)-(d). The expected contributions from the RPV and DGwSL benchmark models are also shown. Figures 2(a) and 2(b) show respectively the jet multiplicity and missing transverse momentum distributions. The latter variable exhibits the strongest discrimination between signal models and SM backgrounds. Both signal benchmark scenarios are incompatible with the data. Figure 2(c) presents the distribution of the SFOS dilepton invariant mass in four-lepton events where this quantity can be reconstructed, before the $E_{\mathrm{T}}^{\mathrm{miss}} > 50$ GeV requirement is applied. Finally, Figure 2(d) shows the distribution of the effective mass variable ($M_{\mathrm{eff}} = E_{\mathrm{T}}^{\mathrm{miss}} + \sum E_{\mathrm{T}}^{e} + \sum p_{\mathrm{T}}^{\mu} + \sum p_{\mathrm{T}}^{\mathrm{jets}}$, for $p_{\mathrm{T}}^{\mathrm{jets}} > 40$ GeV) in all four-lepton events, again before applying the $E_{\mathrm{T}}^{\mathrm{miss}}$ requirement. For all distributions, agreement between data and expected SM backgrounds is observed within uncertainties.

8 Conclusions

A SUSY-motivated search for events with four leptons and missing transverse momentum has been carried out using 2.06 fb^{-1} of $\sqrt{s}$ =7 TeV proton-proton collision data recorded by the ATLAS experiment at the LHC in 2011. With an inclusive selection we observe four events, while 1.7±0.9 are expected from Standard Model processes. Applying a Z boson veto for leptons pairs with the same flavour and opposite charge, we observe no events, while 0.7±0.8 events are expected. Within the selection acceptance, we determine 95% C.L. visible cross-section upper limits for new phenomena of 3.5 fb and 1.5 fb for the selections without and with the Z boson veto, respectively.

Table 3: Number of events in SR1 and SR2 for MC simulation and 2.06 fb^{-1} of 2011 data. SM background expectations listed in this table have been estimated using MC simulation. The uncertainties quoted for the "All" column are inclusive and not the summed uncertainties of the different flavour combinations. Where MC samples yield zero events, the uncertainty is quoted based on the integrated luminosity of the MC sample (see text).

SR1	All	*eeee*	*eeeμ*	*eeμμ*	*eμμμ*	*μμμμ*
$t\bar{t}$	0.17±0.14	0.011±0.042	0.027±0.042	0.09±0.06	0.05±0.07	0±0.018
Single t	0±0.04	0±0.04	0±0.04	0±0.04	0±0.04	0±0.04
$t\bar{t}V$	0.48±0.21	0.072±0.037	0.12±0.06	0.14±0.07	0.08±0.04	0.059±0.032
ZZ	0.44±0.19	0.14±0.08	0.016±0.012	0.21±0.12	0.047±0.032	0.025±0.045
WZ	0.25±0.10	0.015±0.022	0.07±0.04	0.050±0.032	0.11±0.06	0±0.011
WW	0±0.015	0±0.015	0±0.015	0±0.015	0±0.015	0±0.015
$Z\gamma$	0±0.5	0±0.5	0±0.5	0±0.5	0±0.5	0±0.5
Z+(u, d, s jets)	0.33±0.67	0.33±0.67	0±0.29	0±0.29	0±0.29	0±0.29
Z+(c, b jets)	0.024±0.035	0±0.17	0±0.17	0±0.17	0.024±0.035	0±0.17
Drell-Yan	0±0.05	0±0.05	0±0.017	0±0.017	0±0.016	0±0.017
Σ SM	1.7±0.9	0.6±0.8	0.24±0.57	0.5±0.6	0.32±0.55	0.08±0.57
Data	4	0	1	2	0	1

SR2	All	*eeee*	*eeeμ*	*eeμμ*	*eμμμ*	*μμμμ*
$t\bar{t}$	0.13±0.11	0±0.018	0.027±0.042	0.05±0.04	0.05±0.07	0±0.018
Single t	0±0.04	0±0.04	0±0.04	0±0.04	0±0.04	0±0.04
$t\bar{t}V$	0.07±0.04	0.007±0.007	0.024±0.017	0.022±0.021	0.011±0.008	0.005±0.005
ZZ	0.019±0.020	0.008±0.011	0±0.012	0.010±0.018	0±0.012	0±0.012
WZ	0.09±0.05	0±0.020	0.0021±0.0024	0.050±0.032	0.039±0.028	0±0.011
WW	0±0.015	0±0.015	0±0.015	0±0.015	0±0.015	0±0.015
$Z\gamma$	0±0.5	0±0.5	0±0.5	0±0.5	0±0.5	0±0.5
Z+(u, d, s jets)	0.33±0.67	0.33±0.67	0±0.29	0±0.29	0±0.29	0±0.29
Z+(c, b jets)	0.024±0.035	0±0.17	0±0.17	0±0.17	0.024±0.035	0±0.17
Drell-Yan	0±0.05	0±0.05	0±0.017	0±0.017	0±0.016	0±0.017
Σ SM	0.7±0.8	0.35±0.83	0.05±0.57	0.13±0.57	0.12±0.55	0.005±0.567
Data	0	0	0	0	0	0

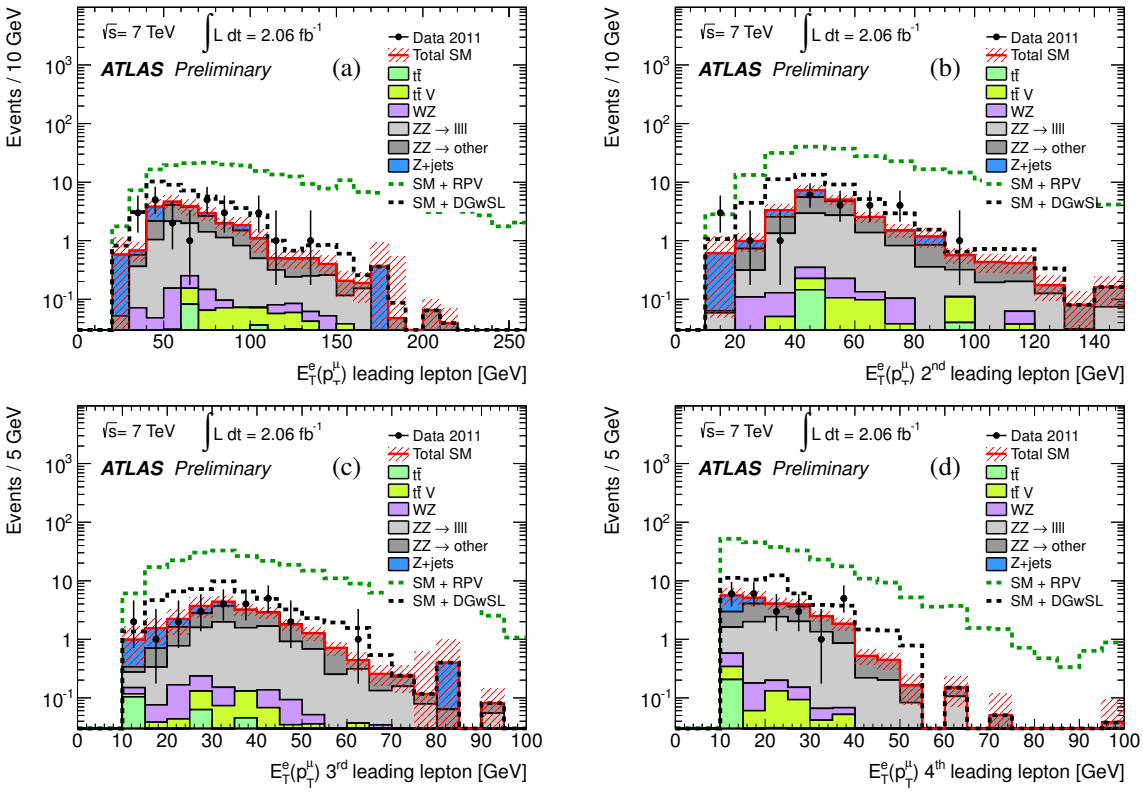

Figure 1: For events with at least four leptons with $E_{\mathrm{T}}^{e}(p_{\mathrm{T}}^{\mu})$ above 10 GeV, the $E_{\mathrm{T}}^{e}(p_{\mathrm{T}}^{\mu})$ distributions of (a) the leading, (b) second-leading, (c) third-leading and (d) fourth-leading lepton are shown for data and MC simulation. The two SUSY benchmark scenarios are also shown. The hatched band represents systematic uncertainties added in quadrature.

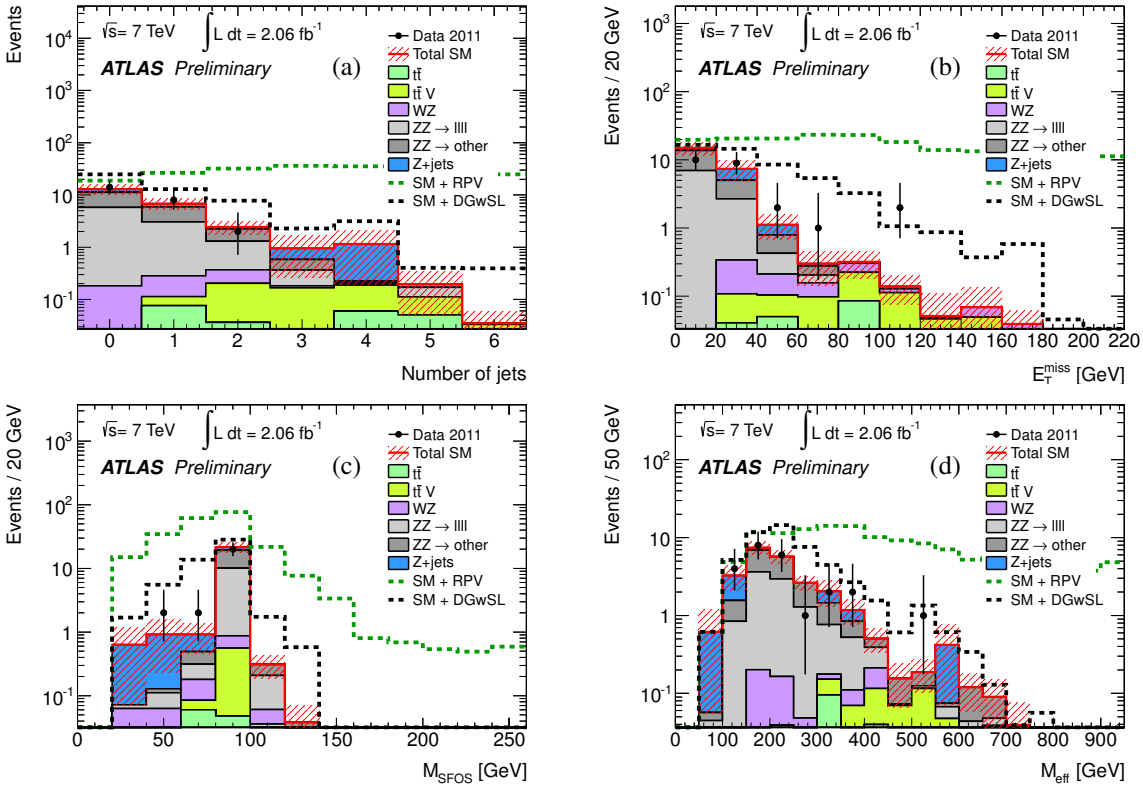

Figure 2: For events with at least four leptons with $E_{\mathrm{T}}^{e}(p_{\mathrm{T}}^{\mu})$ above 10 GeV, distributions of (a) the jet multiplicity, (b) $E_{\mathrm{T}}^{\mathrm{miss}}$, (c) M_{SFOS} and (d) M_{eff} are shown for data and MC simulation. Also shown are the two SUSY benchmark scenarios. In events where multiple SFOS lepton pairs are present, the pair with invariant mass closest to the Z boson mass is plotted in (c). M_{eff} is defined as the scalar sum of the $E_{\mathrm{T}}^{\mathrm{miss}}$, the p_{T} of the leptons and the p_{T} of the jets with $p_{\mathrm{T}} > 40$ GeV in the event. The hatched band represents systematic uncertainties added in quadrature.

References

[1] Y.A. Gol'fand and E.P. Likhtman, JETP Lett. **13** (1971) 323–326.

[2] A. Neveu and J.H. Schwarz, Nucl. Phys. B **31** (1971) 86–112.

[3] A. Neveu and J.H. Schwarz, Phys. Rev. D **4** (1971) 1109–1111.

[4] P. Ramond, Phys. Rev. D **3** (1971) 2415–2418.

[5] D.V. Volkov and V.P. Akulov, Phys. Lett. B **46** (1973) 109–110.

[6] J. Wess and B. Zumino, Phys. Lett. B **49** (1974) 52.

[7] J. Wess and B. Zumino, Nucl. Phys. B **70** (1974) 39–50.

[8] P. Fayet, Phys. Lett. B **69** (1977) 489.

[9] G. Farrar and P. Fayet, Phys. Lett. B **76** (1978) 575–579.

[10] B.C. Allanach et al., Phys. Rev. D. **69** (2004) 115002.

[11] ATLAS Collaboration, ATLAS-CONF-2011-039.

[12] ATLAS Collaboration, ATLAS-CONF-2011-158.

[13] CMS Collaboration, Phys. Lett. B **704** (2011) 411–433; CMS Collaboration, SUS-11-013-PAS; CMS Collaboration, EXO-11-045-PAS.

[14] ATLAS Collaboration, JINST **3** (2008) S08003.

[15] ATLAS Collaboration, Eur. Phys. J. C **70** (2010) 823.

[16] GEANT4 Collaboration, Nucl. Instrum. Meth. A **506** (2003) 250–303.

[17] S. Frixione and B.R. Webber, The MC@NLO 3.2 event generator, arXiv:0601192 [hep-ph], 2006.

[18] P. M. Nadolsky et al., Phys. Rev. D **78** (2008) 013004.

[19] S. Moch and P. Uwer, Phys. Rev. D **78** (2008) 034003.

[20] S. Moch and P. Uwer, Nucl. Phys. Proc. Suppl **183** (2008) 75–80.

[21] N. Kidonakis, Phys. Rev. D **83** (2011) 091503.

[22] N. Kidonakis, Phys. Rev. D **81** (2010) 054028.

[23] M. Mangano et al., JHEP **07** (2003) 001.

[24] ATLAS Collaboration, arXiv:1111.2690 [hep-ex] (Submitted to Physical Review D) (2011).

[25] ATLAS Collaboration, Phys. Lett. B **706** (2012) 295–313.

[26] G. Corcella et al., JHEP **01** (2001) 010.

[27] A. Sherstnev and R. S. Thorne, Eur. Phys. J. C **55** (2008) 553575.

[28] ATLAS Collaboration, ATLAS-CONF-2011-099.

[29] J. Alwall et al., MadGraph/MadEvent v4: The New Web Generation, 2007.

[30] T. Sjostrand, S. Mrenna, and P. Skands, JHEP **05** (2006) 026.

[31] A. Kardos, C. Papadopoulos, Z. Trcsnyi, arXiv:1111.0610 [hep-ph], 2011.

[32] ATLAS Collaboration, JHEP **09** (2011) 072.

[33] J. Butterworth, J. Forshaw and M. Seymour, Z. Phys. C **72** (1996) 637–646.

[34] M. Bahr et al., Eur. Phys. J. C **58** (2008) 639.

[35] B. C. Allanach et al., Phys. Rev. D **75** (2007) 035002.

[36] ATLAS Collaboration, arXiv:1110.3174 [hep-ex] (Submitted to Eur. Phys. J. C) (2011).

[37] M. Cacciari, G.P. Salam, and G. Soyez, JHEP **04** (2008) 063.

[38] ATLAS Collaboration, arXiv:1112.6426 [hep-ex] (Submitted to Eur. Phys. J. C) (2011).

[39] ATLAS Collaboration, ATLAS-CONF-2010-038.

[40] ATLAS Collaboration, Eur. Phys. J. C **71** (2011) 1577.

[41] ATLAS Collaboration, Eur. Phys. J. C **71** (2011) 1630.

[42] ATLAS Collaboration, ATLAS-CONF-2011-116.

[43] U. Langenfeld, S. Moch, and P. Uwer, arXiv:0907.2527 [hep-ph], 2009.

[44] ATLAS Collaboration, Phys. Lett. B **701** (2011) 186–203.

[45] A. L. Read, J. Phys. G **28** (2003) 2693–2704.